Effect of Internal Heating During Hot Compression on the Stress-Strain Behavior of Alloy 304L

M.C. MATAYA and V.E. SACKSCHEWSKY

The temperature change due to the conversion of mechanical deformation to internal heat and its effect on the as-measured stress-strain behavior of alloy 304L was investigated by means of initially isothermal (compression specimen, dies, and environment at same temperature at initiation of test), constant strain rate, uniaxial compression of laboratory-sized cylindrical specimens. Strain rate was varied in the range 0.01 to 1 s^{-1}, where the thermal state of the test specimen varied from nearly isothermal to nearly adiabatic, respectively. Specimens were deformed in the temperature range of 750 °C to 1150 °C to a strain of 1. The change in specimen temperature with applied strain was calculated *via* finite-element analysis (FEA) from the as-measured stress-strain data. Selected predictions were confirmed with embedded thermocouples to verify the model employed. Temperature was found to increase monotonically with strain at a strain rate of 1 s^{-1}, consistent with what is theoretically expected for the adiabatic case. At the 0.1 and 0.01 s^{-1} rates, the sample temperature initially increased, peaked, and then decreased as the sample thinned and the contact area between the sample and the cooler dies increased. As-measured stress was corrected for softening associated with deformational heating by interpolation between the various instantaneous stress-temperature behaviors. The resulting isothermal flow data are compared to those predicted by a conventional method that employs an empirical estimate of the heat retention efficiency of the test specimen, assumed dependent on strain rate but independent of strain, to reduce the increase in temperature calculated for the adiabatic case. Differences between the calculated isothermal stress-strain data from the two methods are discussed. Values for the apparent activation energy of deformation and the strain to the peak in the flow curve, which is associated with the onset of dynamic recrystallization, determined from isothermal stress-strain data differed significantly from those obtained from the as-measured compression test data.

I. INTRODUCTION

UNIAXIAL compression of cylindrical specimens is often used to determine a material's stress-strain (σ-ε) response to plastic deformation at temperatures, strain rates, and to strains typically encountered during conventional hot-working processes such as forging. The σ-ε response yields information about a material's strain-rate sensitivity; work-hardening rate; activation energy for deformation, Q_{DEF}; and equipment loading during forming operations, and it allows upper-bound analysis of metal-working operations. These data are also useful in finite-element analysis (FEA) of metal-forming operations.[1–8]

The accuracy of measured σ-ε data from compression testing is typically degraded by friction between sample and die, causing barreling and nonuniform stress and strain in the sample, and by internal heating of the sample, which typically reduces the flow stress of materials that exhibit thermally activated plastic deformation.[9] Lubrication techniques have been developed to minimize frictional effects. However, as-measured σ-ε curves and associated analysis reported in the literature have often been presented without correction for deformational heating.[10–24]

At high strain rate, $\dot{\varepsilon}$, the heat generated in a test sample is essentially retained during the short duration of the test, and the instantaneous temperature of the test sample, T_i, can be calculated by conventional techniques, without consideration of heat loss to the environment. From sets of σ-ε-T_i data, generated by compression testing at different temperatures, isothermal σ-ε curves can be obtained by interpolation of the σ-T_i data at each increment in ε. Semiatin *et al.*[7] employed this technique to correct as-measured σ-ε curves of Ti-6242 for use in finite-element simulation of metal flow during forging of a turbine disc. Laasraoui and Jonas,[25,26] using a similar technique, showed that correction of the as-measured σ-ε data for internal heating during hot compression testing provided a significantly more precise determination of the static recrystallization kinetics for various low carbon steels.

At low $\dot{\varepsilon}$, the heat of deformation is dissipated, as it is generated, to the surrounding environment, and the test progresses isothermally. In this case, the as-measured σ-ε behavior is also the isothermal behavior. Thus, in the two $\dot{\varepsilon}$ extremes, the bounds of which are determined by test sample geometry and other test conditions that govern heat transfer to the environment, isothermal σ-ε behavior can be obtained rather easily.

In the intermediate $\dot{\varepsilon}$ realm, the process is neither adiabatic nor isothermal, and the calculation of T_i, which is a function of heat transfer from the superheated specimen to the cooler environment (*i.e.*, heat conduction to the dies), is not simple and has not been characterized in detail. Sample temperature can be measured with embedded thermocouples, but testing is complex and

M.C. MATAYA, Associate Scientist, is with EG&G Rocky Flats, Inc., Golden, CO 80402-0464. V.E. SACKSCHEWSKY, formerly Senior Systems Engineer with EG&G Rocky Flats, Inc., is retired.

Manuscript submitted April 19, 1993.

costly, and embedded thermocouples may perturb the σ-ε response of the specimens. To facilitate calculation of isothermal σ-ε curves in this intermediate $\dot{\varepsilon}$ regime, Dadras and Thomas[27] introduced an empirical term, referred to as heat retention efficiency, η, which is used to reduce the temperature rise calculated for the adiabatic case to obtain T_i. The value of η is assumed to vary linearly with log $\dot{\varepsilon}$, $\eta = \eta(\dot{\varepsilon})$, independent of ε.[27,28,29] However, because heat loss from a superheated compression specimen to the dies depends in part on the instantaneous sample geometry (*e.g.*, specimen height and specimen-die contact area), it appears that η must also vary with strain, $\eta = \eta(\dot{\varepsilon}, \varepsilon)$.

Type 304 austenitic stainless steel is a widely used material due to a combination of good corrosion resistance and strength that can be significantly enhanced during forging at elevated temperatures.[30] The flow behavior of 304 and 304L at elevated temperature from a number of investigations has been reviewed by Dadras[31] and Semiatin and Holbrook,[32] and it is apparent that a detailed systematic study of the isothermal flow behavior in the intermediate $\dot{\varepsilon}$ regime at elevated temperatures has not been performed. This type of characterization is needed in order to model processes such as radial forging and press forging, which are characteristically applied during primary and secondary breakdown of commercial ingot material.[33]

The purpose of this investigation was to develop a method to obtain an accurate isothermal σ-ε behavior for 304L at elevated temperature in the intermediate $\dot{\varepsilon}$ realm, where the thermal state of laboratory-sized test specimens is neither isothermal nor adiabatic. Deformational heating of test specimens was studied by performing a thermal-mechanically coupled FEA of the compression test in which the heat of deformation was allowed to dissipate through conduction to the dies. Interpolation of the instantaneous σ-ε-T_i behavior, where T_i is calculated by FEA, was used to determine the isothermal σ-ε behavior. The results are compared to the as-measured test data and to those obtained with the conventional method that employs $\eta(\dot{\varepsilon})$. Values and behaviors of the strain to initiate dynamic recrystallization, ε_p, and apparent activation energy for deformation, Q_{DEF}, obtained from both as-measured and isothermal data are compared and discussed.

II. EXPERIMENTAL PROCEDURE

A. *Material*

The chemical composition of the 304L alloy used in this investigation is given in Table I. The alloy was arc-melted in air and then argon-oxygen decarburized prior to casting a 356-mm-diameter electrode. The electrode was vacuum arc-remelted into a 406-mm-diameter ingot. The ingot was bloomed to a 127-mm, round-cornered square bar on a continuous mill at 1150 °C and hot-rolled to a 38.1-mm-diameter bar. Rolling started at 1100 °C and finished at approximately 900 °C. The bar was swaged at room temperature to a 15.2-mm-diameter rod. The rod was solution heat-treated at 1000 °C for 1 hour and water-quenched, providing the starting material for the investigation. Prior study of this heat of 304L showed that this particular solution heat treatment produces a well-annealed, relatively dislocation-free matrix with equiaxed grains having an average grain diameter of 0.038 mm.[30]

Table I. Chemical Analysis of 304L Alloy

Element	Analysis (Mass Pct)
Cr	18.6
Mn	1.9
Ni	10.0
P	0.011
Si	0.57
Mo	0.055
Co	0.077
C	0.022
S	0.0003
N	0.015
Fe	balance

B. *Elevated Temperature Compression Testing*

The test setup is shown schematically in Figure 1. Compression testing was accomplished in a 250 KN servohydraulic testing machine (manufactured by M.T.S. Corp., Minneapolis, MN) outfitted with an electric resistance clam-shell furnace. The vertical load column was composed of two opposing ASTROLOY* rams, which were hollowed to facilitate heating, and flat smooth (lapped to 8 rms surface finish with opposite faces parallel to within 0.0127 mm over a 69.85-mm diameter) SiN compression dies, fitted to the end of the rams. Cylindrical compression samples, 12.7-mm diameter by 19.05-mm high, were machined from the heat-treated 15.1-mm-diameter rod, with specimen axis parallel to rod axis. The end faces were recessed to form a lubricant well, an effective technique for constraining lubricant to the sliding face during compression.[34] Weis[35] verified the effectiveness of this technique compared to others and determined an optimum well geometry for the specimen used in this investigation (lower right in Figure 1). Various glass lubricants were employed to accommodate the wide range of testing temperatures: Delta Glazes No. 13 for 750 °C, No. 93 for 850 °C, No. 349M for 950 °C, and No. 347M for 1050 °C and 1150 °C (products of Atcheson Chemical Co., Port Huron, MI). The combination of hard smooth dies, lubricant well geometry, and glass lubricant provided excellent lubrication for the duration of the compression test, demonstrated by the absence of barreling of the free surface on the compressed test sample (Figure 2). Test specimens were loaded onto the bottom die in the furnace in air, held for 10 minutes at the test temperature (specimens required approximately 5 minutes to equilibrate), compressed uniaxially to a strain of 1, and quenched in water immediately after deformation. The time to quench was between 1 and 2 seconds. Test temperatures varied between 750 °C and 1150 °C. The initial grain size was found to be stable

*ASTROLOY is a trademark of Geneva Electric Company, Sun Valley, CA.

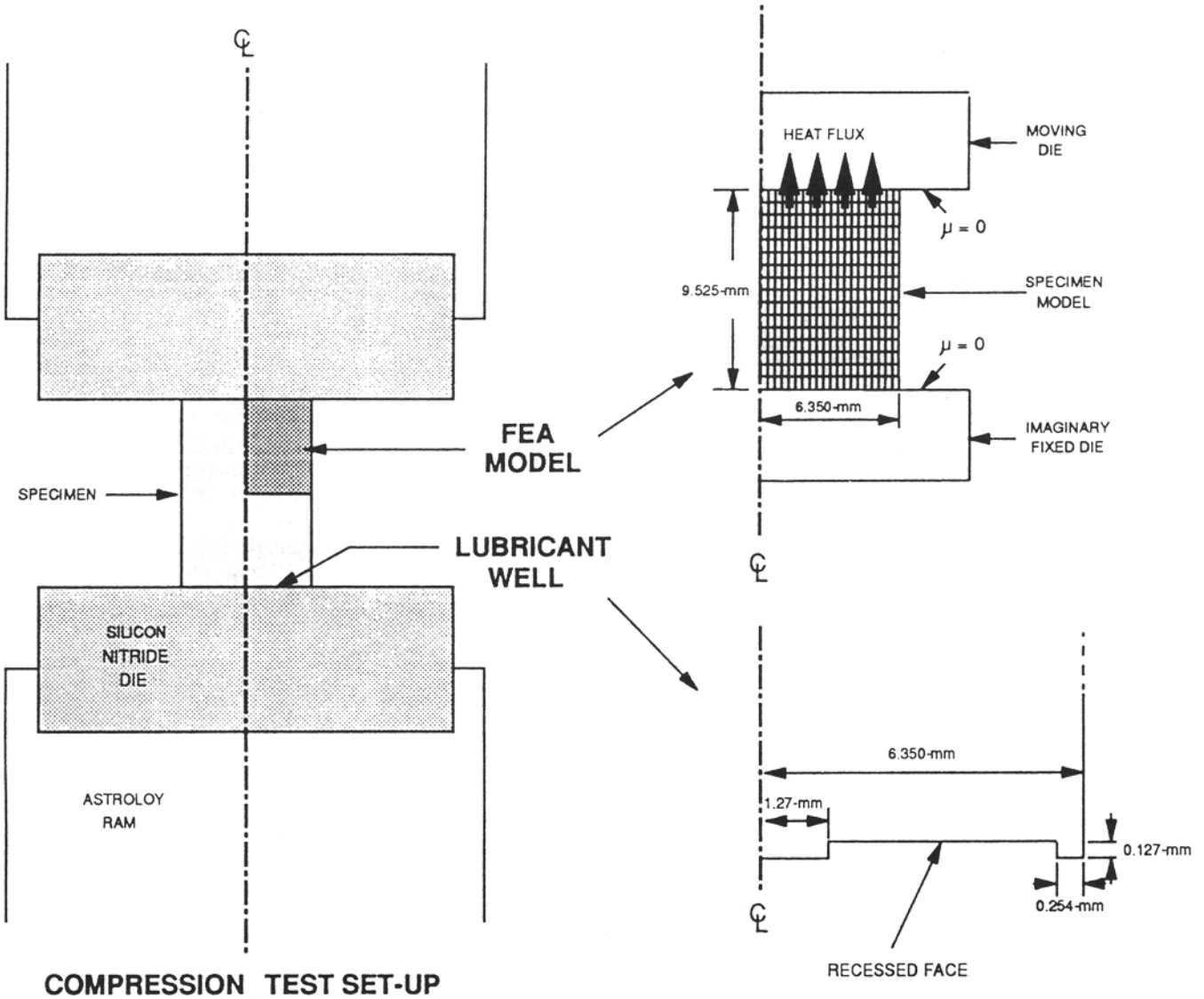

Fig. 1—Schematic of compression test setup, FEA model, and lubricant well on compression test specimen.

during preheating in the 750 °C to 1050 °C range. The average grain diameter increased from 0.040 to 0.120 mm during the 1150 °C preheat cycle. The effect of this increase on the results is considered. The velocity of the moving die was varied by computer control in order to apply deformation at a constant $\dot{\varepsilon}$ of 0.01, 0.1, or 1 s^{-1}. Compliance in the load train resulted in deviations in ε and $\dot{\varepsilon}$ up to about −5 pct with the maximum occurring at the lowest temperature, at which the greatest loads were encountered.

The true flow stress σ can be assumed equal to the true average pressure because the coefficient of friction between sample and die is near zero (Figure 2).[36] In addition, the strain distribution can be assumed uniform throughout the specimen, and true strain ε can be calculated from the change in test specimen height.[37] Note for uniform uniaxial compression, the effective or significant stress and strain reduce to the axial normal component of stress and strain, as is the case for tensile testing in the uniform elongation realm.[37] Values for σ and ε were calculated from the as-measured load and

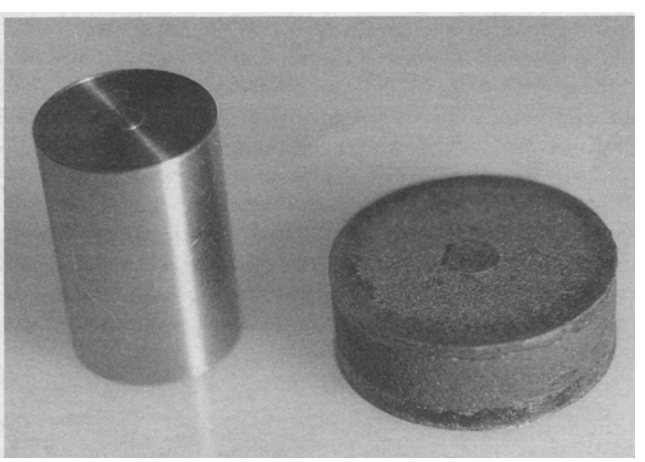

Fig. 2—Compression test specimen prior to deformation (left) and a typical deformed specimen (right).

corrected displacement data using conventional relationships.[37] Sample dimensions, measured at ambient temperature, were corrected for thermal expansion that occurs on heating to the test temperature T_0. The measured displacement of the sample, obtained with a linear-variable-differential transformer (LVDT) mounted at the lower end of the moving ram, was corrected for test system compliance. Calculated values of final ε, obtained from the LVDT displacement and corrected for compliance and for cooling to ambient temperature, were typically within 1 to 2 pct of the measured plastic strain, calculated from the actual initial and final height of the test sample.

Sample heating during deformation was measured on selected samples with an embedded thermocouple located at the specimen center (midheight and mid-diameter). The thermocouple was a sheathed type K with an exposed, beaded junction. Sheath material was type 304 stainless steel. Sheath, bead, and wire diameters were 1.57, 0.7, and 0.25 mm, respectively. The time constant to reach 62.3 pct of a stepped increase in temperature was approximately 0.45 seconds. In this study, embedded thermocouples were found to have a negligible effect on the flow curves, determined by comparing the results from samples with and without thermocouples.

C. *Determination of Isothermal Stress-Strain Behavior*

1. *An empirical analysis*

The as-measured σ-ε data were corrected for deformational heating by two different techniques. The first, discussed in this section, employs the empirical term η[27] to estimate T_i, the instantaneous temperature at the midheight position of the compression specimen, and is hereafter referred to as the empirical analysis (EA) method. It consists of calculating the change in sample temperature, ΔT, with applied ε by the following conventional relationship:

$$\Delta T = (\eta k/\rho C_p) \int_0^{\varepsilon_f} \sigma \, d\varepsilon \qquad [1]$$

where ρ is density, C_p is heat capacity per unit mass (where $C_p = C_p(T)$), ε_f is the final true plastic strain, k is a mechanical energy-to-heat conversion factor, and η is the fraction of deformational energy that appears as a temperature rise. Based on the measured value of T_i at an applied ε of 0.7, determined from an embedded thermocouple located at the midheight-midradius location, in cylindrical compression samples of aluminum alloy 2024 compression samples strained at various rates,[28] it has been suggested that η varies linearly with the logarithm of $\dot{\varepsilon}$, equaling 0 at 0.001 s^{-1} or less and 0.95 at 1.0 s^{-1} or greater.[29] Following this suggestion, the value of η is expressed as follows:

$$\eta = (0.316) \log_{10} \dot{\varepsilon} + 0.95 \qquad [2]$$

Values for ΔT were calculated, *via* Eqs. [1] and [2], for each measured increment of ε, approximately 0.005. The trapezoid rule was used for the integration in Eq. [1]. For adiabatic conditions, η is usually assumed to be between 0.9 and 0.95. The latter value is assumed in the EA method.

Next, $(\sigma, T_i)|_{\dot{\epsilon}}$ relationships were constructed from the as-measured σ-ε data for different T_0, where $T_i = T_0 + \Delta T(\varepsilon)$, and at regular increments of ε. Finally, at a given value of ε and T_0, the softening, $\Delta\sigma$, due to ΔT was calculated, assuming a linear variation of log σ with $1/T_i$, and added to the as-measured value of σ to obtain the isothermal value.[29]

2. *A method using FEA*

An alternative method for estimating T_i from as-measured σ-ε data was developed in this study. It uses FEA to calculate the T_i in the compression sample with increasing ε. Isothermal σ-ε data are then determined by interpolation to T_0, similar to the EA method. The FEA model employs the as-measured σ-ε curve and the relevant physical properties analogous to Eq. [1]. However, as the FEA calculation progresses incrementally with ε, effects of the changes in sample geometry on heat flow to the dies are automatically included in the transient temperature calculations. Thus, FEA essentially replaces Eq. [1], adding effects of geometry changes (*i.e.*, ε), which are absent in the η term in that equation. The method is summarized briefly here and discussed in detail below.

Step 1. Frictionless compression test gives $\sigma = \sigma(\varepsilon)|_{\dot{\epsilon}}$ for each test $\dot{\varepsilon}$ and each initial test temperature T_0.[36]

Step 2. Input the as-measured $\sigma = \sigma(\varepsilon)|_{\dot{\epsilon}}$ from a single test as the material behavior into the FEA model and calculate instantaneous sample temperature, T_i, at specimen center for that test. Repeat for each compression test. This yields $\sigma = \sigma(\varepsilon, T_i)|_{\dot{\epsilon}}$ for each initial test condition. Note, this step is analogous to the EA calculation in Eq. [1] with η replaced by FEA calculation of the heat flow to the die.

Step 3. Obtain $\sigma = \sigma(\varepsilon)|_{T_0,\dot{\varepsilon}}$ for each T_0 and $\dot{\varepsilon}$ by interpolation between appropriate sets of $\sigma(\varepsilon, T_i)|_{\dot{\epsilon}}$ at regular increments of ε.

Figure 1 shows a schematic of the finite-element model used to simulate the compression tests. The MARC* finite-element code was used for the simulation. The analysis was elastic-plastic and thermal-mechanically coupled. Values of σ, ε, and T_i were calculated for each time increment during the simulation, where T_i is taken at the specimen center. The analysis assumes symmetry about the center axis, oriented in the vertical direction in Figure 1 and in the test setup, and about a perpendicular plane through the midheight of the cylinder. Axial symmetry implies that the system can be represented by a two-dimensional model. Vertical symmetry implies that only one-half of the cylinder must actually be modeled. Thus, the model consists of one quadrant of a vertical cross section through the cylinder, as shown in Figure 1. The quadrant of the 12.7-mm diameter by 19.05-mm high (0.5 × 0.75 in.) cylindrical test sample is represented by a mesh of 20 four-node

*MARC is a trademark of MARC Analysis Research Corp., Inc., Palo Alto, CA.

quadrilateral elements in the radial direction and 16 elements for the half-height. The conversion of mechanical energy to heat was assumed to have an efficiency of 0.95, consistent with the value assumed in the EA method.

The upper die of the compression test setup is represented by the upper rigid die in Figure 1. Simulated movement of this die was controlled by a subroutine within the FEA code to provide a specified constant $\dot{\varepsilon}$.

A friction coefficient of zero was used between the die and the cylindrical test specimen, based on the observed lack of barreling (Figure 2) on the free surface of compressed samples. For frictionless compression, the as-measured σ-ε behavior, which is an average for the sample, can be assumed, according to Rowe,[36] to be equal to the true material behavior, because ε and $\dot{\varepsilon}$ are uniform throughout the compression sample. Thus, the as-measured behavior was used to approximate the true material behavior throughout the test sample in the FEA model (Step 2). In both EA (conventional) and FEA, the sample temperature reference is located at the midheight of the sample. In the EA technique, temperature is measured *via* thermocouple at the midheight, at a strain of 0.7. In the FEA technique, the sample temperature at the midheight is calculated, considering heat flow to the dies, as strain increases. The temperature in the sample may vary from center to die surface, due to heat conduction from the sample, heated by deformation, to the slightly cooler die. Because the as-measured stress-strain behavior, which is an average behavior for the sample, is matched with the temperature at the sample midheight, which may be greater than the average temperature in the test sample, an associated error may be introduced during interpolation to isothermal conditions. For example, the temperature in a test sample 1 mm from the compression surface during the 850 °C, $\dot{\varepsilon} = 0.1\ s^{-1}$ test was measured to be 868 °C at a strain of approximately 0.8 compared to 874 °C at the midplane. This difference is relatively small, 6 °C, and apparently had little effect on sample geometry (barreling should be observed if significant die chill is coupled with an inverse temperature dependence of the flow stress). If an average temperature is assumed, T_i for this test is approximately 871 °C, rather than 874 °C (value at midheight), and the estimated isothermal flow stress would be reduced slightly from the value calculated assuming T_i at the sample midheight (approximately 265 *vs* 268 MPa from the data subsequently provided in Table IV).

Heat transfer due to conduction between the test specimen and die is included in the analysis to allow the heat generated in the specimen by deformation to be dissipated into the die, which acts as a constant temperature heat sink. For this analysis, T of the moving rigid die is set equal to the initial temperature of the test specimen, T_0. The lower rigid die shown in the model is an imaginary die through the specimen midplane (Figure 1), and its function in the model will be discussed. Temperature-dependent values of elastic modulus, thermal expansion coefficient, thermal conductivity, and specific heat used in the FEA model are listed in Table II.

The coefficient of heat transfer between the specimen and die was determined by matching FEA-predicted variations of ΔT with ε for various assumed values of the heat-transfer coefficient to a measured variation (*via* embedded thermocouple) obtained at 950 °C and a $\dot{\varepsilon}$ of $0.1\ s^{-1}$, as shown in Figure 3. Preliminary FEA analyses, not shown here, revealed that the temperature profile was most sensitive to the film coefficient for this particular combination of deformation parameters. Based on this figure, the coefficient was assumed to be $6.54 \times 10^3\ J/s/m^2/K$ (curve C). This value is lower, by a factor of approximately 2, than what is typically experienced in conventional forging of steel with graphite-based lubricants.[38] The lower value encountered in this study could be due to greater insulating qualities of the glass lubricants used in this study, compared to the graphite-based and other lubricants that are typically used in forging, and/or due to the use of a lubricant well on the ends of the specimens, which serves to maintain a relatively thick and continuous film of lubricant between the specimen and the dies for the duration of the test. A higher value for the coefficient might have been assumed considering that a variable die temperature in the FEA model should produce predicted curves (for Figure 3) which show less effect of die chilling at high strain. In this case, it appears that the value of the coefficient selected from Figure 3 may be greater than was assumed in this study.

Figure 4 shows the variation of as-measured ΔT, $T_i - T_0$, with ε, acquired from thermocouples embedded in test specimens, and the corresponding EA and FEA predicted curves. The FEA curves closely approximate the measured behavior, giving validity to the FEA model. The as-measured and FEA results show some difference because of a number of assumptions made in the FEA method and for the as-measured data. For example, some of the heat of deformation conducted from the specimen to the dies as the test proceeds will result in a slight heating of the dies; and therefore, slightly less heat will be transferred to the dies than predicted by FEA because of the assumption of a constant temperature for the moving rigid die. In this case, the as-measured sample T_i would be expected to lie slightly above the FEA T_i (the opposite is observed in Figure 4) and should increase with strain at a greater rate (observed in Figure 4). A number of other assumptions may have caused the FEA T_i to exceed the as-measured T_i. First, the effects of radiative and convective cooling were neglected in the FEA model, because calculations indicated that their effects on T_i would be relatively small compared to conduction effects (for example, the ratio for rate of heat dissipation by radiation to the rate of heat generation within the sample was less than 0.05). If incorporated in the FEA model, however, T_i would certainly be reduced a finite amount, and the FEA curves in Figure 4 would be lowered. Second, the lag in the as-measured temperature due to the thermocouple time constant (0.45 seconds for a 63.2 pct response) was neglected in the analysis. If a correction were applied, estimated to be on the order of 0.05 ε, the as-measured curve would shift to the left, effectively raising the as-measured curve relative to the FEA curve in Figure 4. Finally, it was assumed that mechanical work was converted to heat with a 95 pct efficiency, consistent with the EA method. The efficiency is generally assumed to

Table II. Variation of Young's Modulus, Thermal Expansion Coefficient, Thermal Conductivity, and Specific Heat with Temperature and Other Constants Used in the FEA Model*

T (°C)	Young's Modulus (MPa) ($\times 10^5$)	Thermal Expansion Coefficient (cm/cm °C) ($\times 10^{-5}$)	Thermal Conductivity (cal/s cm °C) ($\times 10^2$)	Specific Heat (cal/g °C)
−17.8	1.994	1.507	3.52	0.089
93.3	1.912	1.613	4.02	0.090
204.4	1.830	1.699	4.34	0.091
315.6	1.749	1.768	4.68	0.093
426.7	1.667	1.823	4.96	0.095
537.8	1.585	1.868	5.29	0.098
648.9	1.504	1.908	5.66	0.104
760.0	1.422	1.946	6.00	0.109
871.1	1.340	1.980	6.32	0.113
982.2	1.258	2.011	6.66	0.115
1093.3	1.177	2.034	6.98	0.117

Other constants:

Density:	7.999 g/cm^3
Poisson's ratio:	0.300
Mechanical energy to heat:	
Conversion:	0.238978 cal/MPa cm^3
95 pct efficiency:	0.227029 cal/MPa cm^3

*Sources: Department of Defense specification MIL-HDBK-5D, 2-192; Aerospace Structural Metals Handbook, AFML-tr-68-115, 1974, code 303, p. 27.

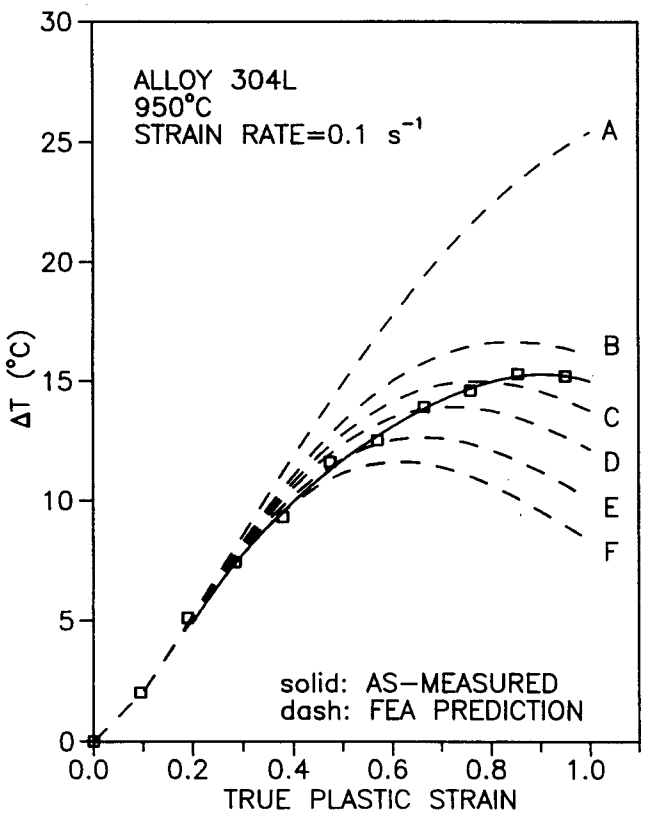

Fig. 3—The change in specimen temperature with true plastic strain for alloy 304L compressed at 950 °C and a $\dot{\varepsilon}$ of 0.1 s^{-1}. Both the as-measured (solid) and FEA (dashed) curves are shown. Curves A through F were generated with heat transfer (film) coefficients of 1.635, 4.905, 6.540, 8.175, 11.44, and 16.35 × 10^3 J/s/m^2/K, respectively. As-measured temperature data were obtained from an embedded thermocouple located at the center of the specimen.

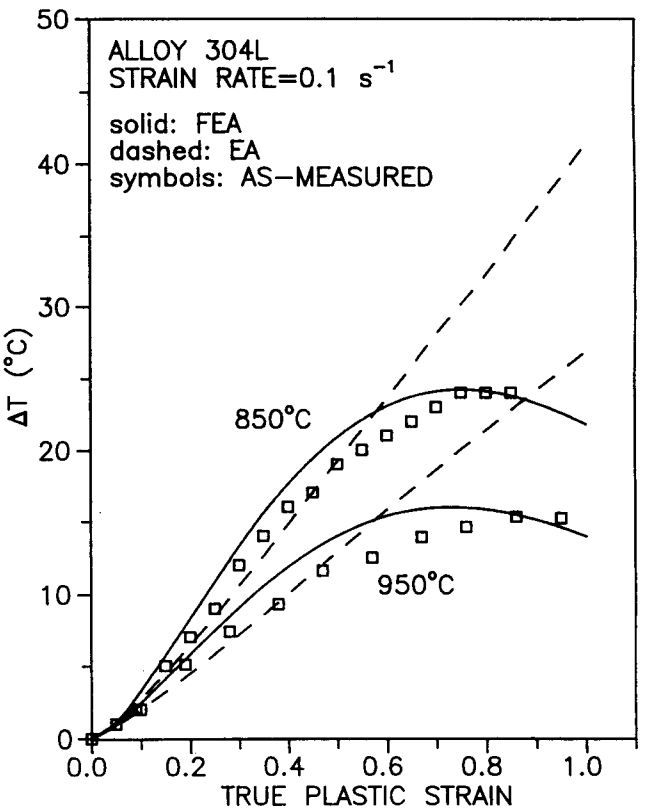

Fig. 4—The change in specimen temperature with true plastic strain for alloy 304L compressed at a $\dot{\varepsilon}$ of 0.1 s^{-1}, at temperatures of 850 °C and 950 °C. Dashed curves were calculated by the EA method and solid curves by FEA. The open symbols (squares) were measured with an embedded thermocouple located at the center of the test specimen.

be in the 90 to 95 pct range. Assuming a lower value in the analysis, *e.g.*, 90 pct, would reduce deformational heating and lower the FEA curves in Figure 4 relative to the as-measured curves. Although some errors are introduced in both FEA and as-measured data, the approximate equivalency, in magnitude and behavior with ε, between the two sets of data demonstrates that FEA provides a better approximation for T_i than does EA.

The heat-transfer coefficient between the sample and die was assumed to be constant; however, as the test proceeds, the lubricant barrier thins and microscopic contact areas may increase, causing the actual coefficient to increase. Assumption of a constant average coefficient will cause some underestimation of ΔT at low ε and overestimation at high ε.

Separate FEA analyses were run to simulate each combination of T_0 and $\dot{\varepsilon}$ employed experimentally. For each case, the corresponding as-measured σ-ε data was used as the specimen flow stress behavior for FEA, and the evolution of the T_i profile within the specimen was calculated. In essence, the FEA method is the same as that implied by Eq. [1], except that a better estimate of the effect of the η term is made by including a model of the cylinder and die, which considers effects of the film coefficient, geometry change (ε), and $\dot{\varepsilon}$ on the heat flow across the cylinder-die interface.

Initial FEA analyses showed a slightly nonuniform distribution of σ within the deformed cylinder due to nonuniform T within the cylinder and the associated thermal stresses from the temperature-dependent coefficient of thermal expansion (Table II). Thus, the desired σ-ε-T_i data could not be simply extracted from any one arbitrary FEA element in the cylinder, as would be the case for a perfectly uniform distribution of stress. The lower, stationary rigid die, shown in the model (Figure 1), was introduced to provide an independent calculation of σ. Values of σ are obtained by dividing the load on the lower rigid die (a standard quantity calculated by the FEA code) by the area at midheight, obtained by tracking the position of the outer node on this plane. For the lower imaginary die, the friction and film coefficients were assumed to be zero, because material located at the positions of these nodes in the test specimen was not actually subjected to frictional forces nor was there heat flow across the midplane of the test specimen. Strain was taken as the average of the minimum and maximum equivalent plastic ε calculated in the cylinder (a commonly supplied result of the FEA code). Typically, the two extremes of equivalent plastic strain were within 1 to 2 pct of each other. Temperature, T_i, was taken from the node located at the specimen center. As would be expected from the model, the temperature was found to be constant in the radial direction.

The FEA output gives a set of σ-ε-T_i for each test at values of ε, which are nonuniformly spaced. New sets were determined at 0.01 increments of ε by linear interpolation. For constant $\dot{\varepsilon}$, isothermal σ-ε curves for each T_0 were then obtained by linear interpolation at regular increments of ε between the five sets of σ-ε-T_i data corresponding to the five T_0 (750 °C to 1150 °C) used in testing. For interpolation, σ was assumed to vary in a piecewise linear manner with T_i at constant ε, rather than log σ with $1/T_i$, because plots (not shown) demonstrated this to be the better method for a majority of the corrections, particularly for T_0 = 750 °C, where ΔT is large and extrapolation below successive temperatures used to generate the isotherms, rather than interpolation between successive temperatures, was required. Based on a study of the data, the log σ-$1/T$ method was judged to overstate the correction because of the nearly linear behavior of σ with T_i in this temperature regime. This process, repeated for each $\dot{\varepsilon}$, gives $\sigma = \sigma(\varepsilon)|_{T_0,\dot{\varepsilon}}$.

III. RESULTS

A. *Test Specimen Temperature Behavior*

Figures 5, 6, and 7 show the calculated ΔT, $T_i - T_0$, with applied ε for compression samples deformed at a $\dot{\varepsilon}$ of 1, 0.1, and 0.01 s^{-1}, respectively. Both predictions, EA (dashed curves) and FEA (solid curves), are shown. In general, ΔT increases as deformation temperature, T, decreases, because in Eq. [1], σ varies inversely with T. For example, Figure 5 shows that ΔT is approximately 80 °C and 20 °C for the 750 °C and 1150 °C tests conducted at a $\dot{\varepsilon}$ of 1 s^{-1}. In this figure, the FEA curves lie below the corresponding EA curves, because FEA predicts a finite amount of heat conduction to the SiN dies, whereas at this $\dot{\varepsilon}$, the EA analysis assumes η to be equal to its maximum value, 0.95, which defines the thermal state of the compression sample to be purely adiabatic.

Figures 6 and 7 show that as ε increases, ΔT from FEA rises rapidly, peaks, and then decreases. The drop

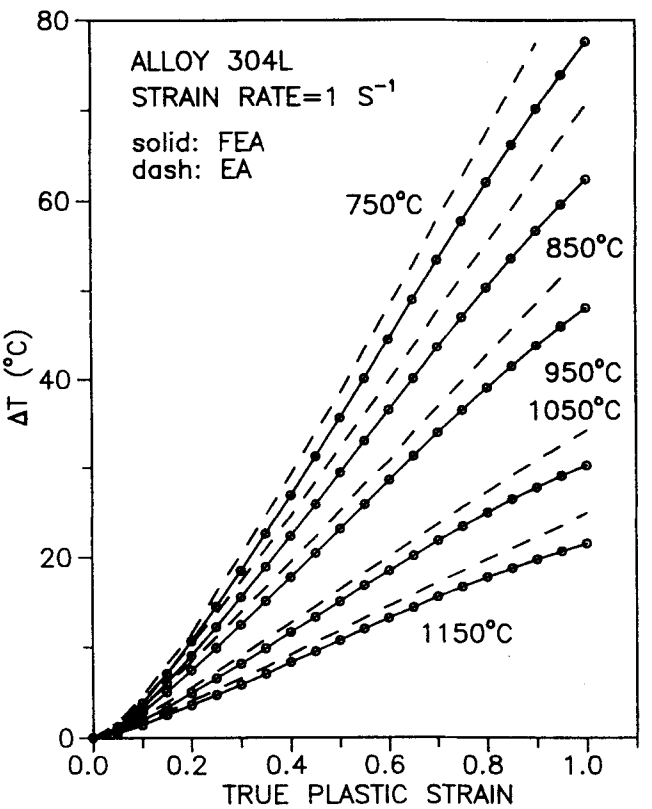

Fig. 5—The change in specimen temperature with true plastic strain for alloy 304L compressed at a $\dot{\varepsilon}$ of 1 s^{-1}. The initial test temperatures, between 750 °C and 1150 °C, are shown. Dashed curves were calculated by the EA method and the solid curves by FEA.

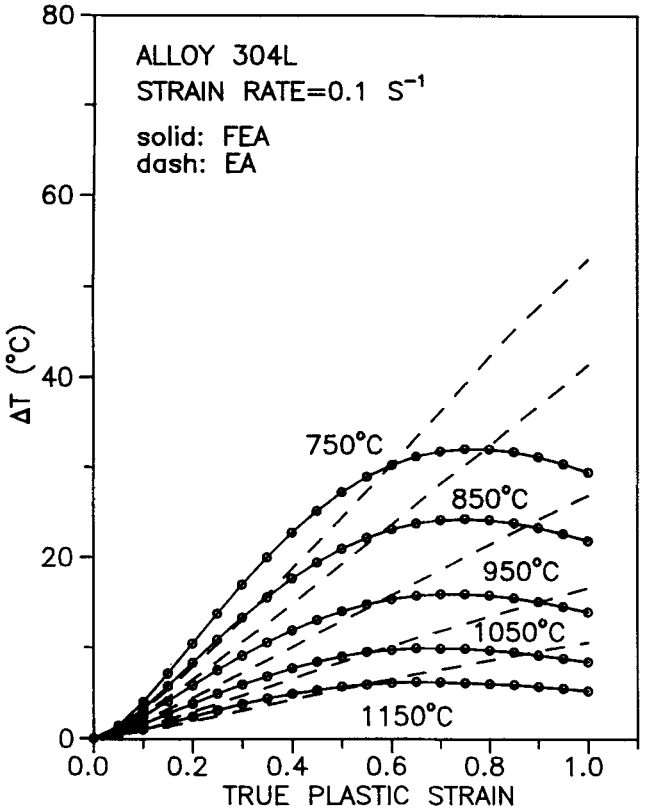

Fig. 6—The change in specimen temperature with true plastic strain for alloy 304L compressed at a $\dot{\varepsilon}$ of 0.1 s^{-1}. The initial test temperatures, between 750 °C and 1150 °C, are shown. Dashed curves were calculated by the EA method and solid curves by FEA.

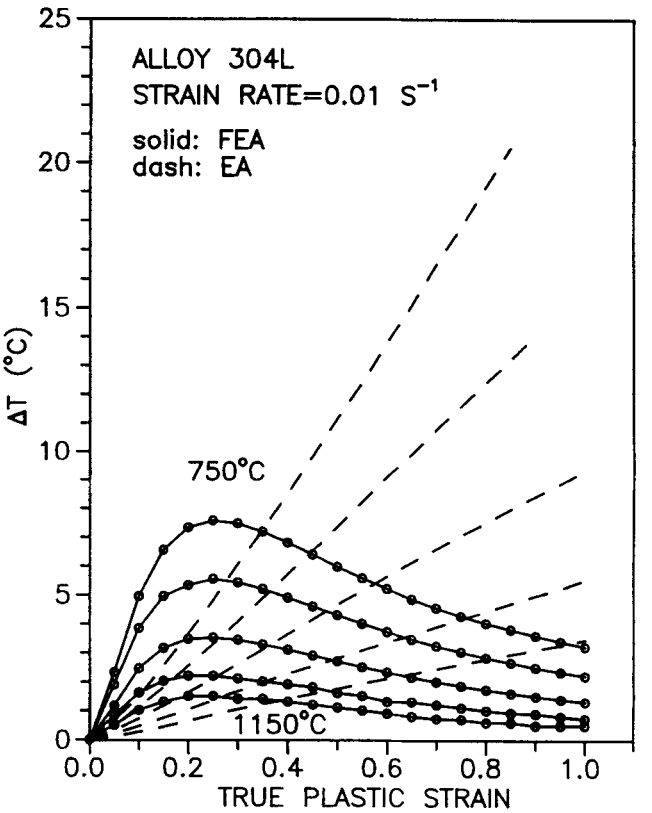

Fig. 7—The change in specimen temperature with true plastic strain for alloy 304L compressed at a $\dot{\varepsilon}$ of 0.01 s^{-1}. The initial test temperatures, between 750 °C and 1150 °C, are shown. Dashed curves were calculated by the EA method and solid curves by FEA.

in ΔT is attributed to the changing sample geometry as the test progresses. The reduction in sample height (or thickness) decreases the distance from the center of the sample to the die face. This, in turn, increases the T_i gradient and hence the heat flow. Secondly, the sample increases in diameter. The contact area between the specimen and die increases causing an increase in heat flow as deformation proceeds. Equation [1], used in the EA method, predicts monotonic increases in temperature, as shown in the figures.

Figures 6 and 7 also show that at low ε, the magnitude of ΔT from FEA is greater than from EA, and at high ε, it is less. The increase in EA ΔT with ε from Eq. [1] is moderated only by η, which is assumed independent of ε. Actually, η varies significantly with ε, as will be demonstrated. Because η was approximated from measurements of ΔT after the application of a relatively high ε, 0.7,[28,29] η represents the average heat retention behavior of a changing sample geometry for the ε range from 0 to 0.7. Thus, the calculated value of η is actually too low at low ε, resulting in anomolously low ΔT, and too high at high ε, resulting in anomolously high ΔT, as shown in Figures 4, 6, and 7.

B. *As-Measured and Isothermal Stress-Strain Behavior*

Figures 8, 9, and 10 show the as-measured and the calculated (FEA) isothermal σ-ε curves for temperatures between 750 °C and 1150 °C and strain rates of 1, 0.1, and 0.01 s^{-1}, respectively. Values for σ at regular increments of $\varepsilon = 0.1$ are provided in Tables III through V. In each case, the as-measured curves lie below the predicted isothermal curves because of the flow softening associated with deformational heating in the test sample. Comparison of the figures and tables shows that the difference between the as-measured and isothermal curves increases with increasing $\dot{\varepsilon}$ and decreasing T. For example, at the greatest $\dot{\varepsilon}$ (1 s^{-1}) and the lowest T_0 (750 °C), the corresponding values of σ at $\varepsilon = 1$ are 358 (as-measured), 430 (FEA isothermal), and 486 MPa (EA isothermal). An increase in $\dot{\varepsilon}$ allows less time for heat transfer from the superheated specimen to the dies, and the greater resulting ΔT induces relatively more softening in the measured behavior. Decreasing T gives greater σ and then a larger ΔT from Eq. [1]. At the lowest $\dot{\varepsilon}$ and highest T_0, very little correction is needed, and the as-measured curves are equal to the calculated isothermal behavior.

The as-measured behavior for 304L in this study is in excellent agreement with the as-measured flow curves for 304L reported by Semiatin and Holbrook[32] for testing conditions of $\dot{\varepsilon} = 0.01$ s^{-1} and T_0 values of 800 °C and 1000 °C and those of Barraclough and Sellars[39] for 304 at $\dot{\varepsilon} = 1$ s^{-1} and 950 °C, 1050 °C, and 1150 °C. However, as-measured 304 flow curves from Suzuki *et al.*[40] for $\dot{\varepsilon} = 0.2$ and 0.8 are relatively low at $T_0 =$ 800 °C and high at 1200 °C compared to the results presented here.

Softening due to deformational heating changes the

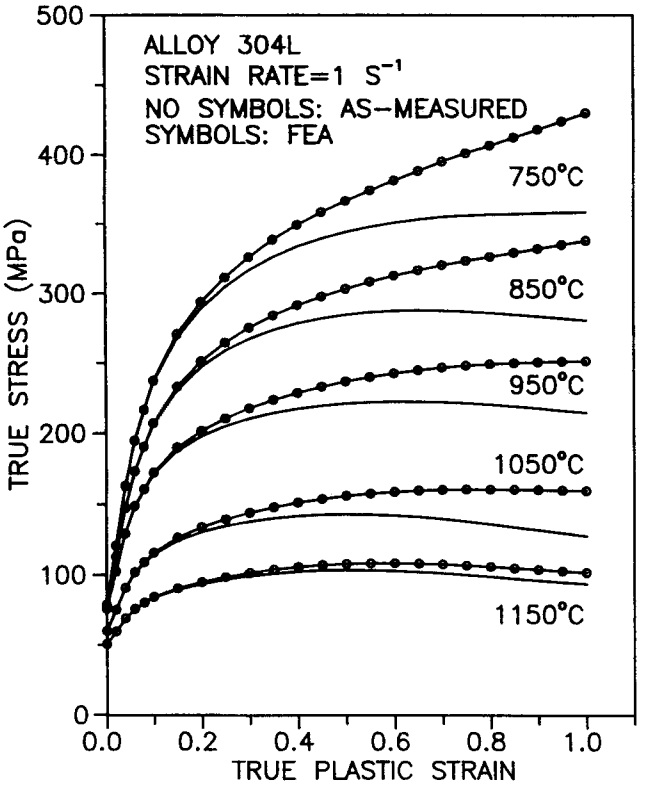

Fig. 8—True stress *vs* true plastic strain for alloy 304L compressed at a $\dot{\varepsilon}$ of 1 s^{-1}. The initial temperature of the tests ranged between 750 °C and 1150 °C. Curves without symbols are the as-measured behaviors. Curves with symbols (circles) are the predicted isothermal behaviors from the FEA method.

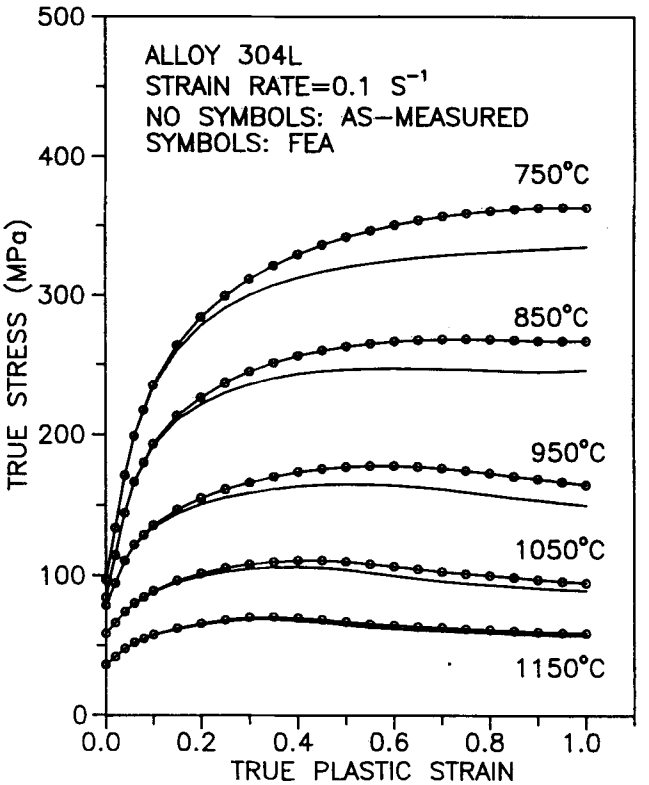

Fig. 9—True stress *vs* true plastic strain for alloy 304L compressed at a $\dot{\varepsilon}$ of 0.1 s^{-1}. The initial temperature of the tests ranged between 750 °C and 1150 °C. Curves without symbols are the as-measured behaviors. Curves with symbols (circles) are the predicted isothermal behaviors from the FEA method.

shape of the flow curves. Many of the as-measured curves exhibit initial hardening followed by softening. The softening behavior apparent in the as-measured 950 °C and 1050 °C curves in Figure 8 is consistent with that observed from the as-measured curves of Barraclough and Sellars.[39] The position of the transition or peak in the flow curve is often associated with the onset of dynamic recrystallization, which was observed for this particular 304L material[30] (Figures 23 and 24 in Reference 30), and has been related to the apparent activation energy for deformation.[41,42] Correcting the as-measured curves shifts the value of ε at the peak, ε_p, to significantly higher values, as shown in Table VII. For example, for $\dot{\varepsilon} = 1\ s^{-1}$ and $T_0 = 950$ °C, the as-measured $\varepsilon_p = 0.6$, whereas the FEA $\varepsilon_p > 1$.

The observed differences between the FEA and EA values of σ in Tables III and IV are due primarily to the difference in calculated ΔT. The EA method generally gives greater values of ΔT (Figures 5 through 7) and thus greater values of σ correction. An exception occurs at the lower strain rates and at relatively low ε, *e.g.*, $\varepsilon = 0.2$. Here, the EA ΔT is slightly less than the FEA ΔT, and the data in the Tables IV and V show that the EA isothermal σ values are slightly less than the corresponding FEA values. The overcorrection by the EA method at high ε also changes the shape of the flow curve, shifting the peak to higher values of ε. For example, for test conditions of $\dot{\varepsilon} = 0.01\ s^{-1}$, $T_0 = 850$ °C, and of $\varepsilon = 1$, the FEA $\varepsilon_p = 0.6$ (Table VII), whereas EA $\varepsilon_p > 1$ (from the behavior in Table V).

In addition to differences in ΔT from the two correction methods, the magnitude of $\Delta\sigma$ correction is also affected by the assumed relationship between σ and T, a linear σ-T relationship in FEA and a linear log σ-$1/T$ relationship in EA. Because the data does obey a near linear relationship between σ and T, especially at low T, the EA method results in a larger correction for $T_0 = 750$ °C than would be anticipated for the calculated ΔT, because the correction is obtained by extrapolation of the log σ-$1/T$ relationship to a temperature (750 °C) significantly outside the range (774 °C to 865 °C) used to define the relationship. A modified EA method, EA-MOD, employing a linear σ-T relationship is introduced here to further examine the σ correction calculated by the EA method. For $\dot{\varepsilon} = 0.01\ s^{-1}$, $T_0 = 750$ °C, and $\varepsilon = 1$, Table V shows that the corresponding values of $\Delta\sigma$ from the three methods are 3 (FEA), 47 (EA), and 30 MPa (EA-MOD). Comparing the two methods employing a linear σ-T relationship, a 10-fold difference in ΔT, 2.3 °C (FEA) compared to 24 °C (EA, EA-MOD) shown in Figure 7, results in a 10-fold difference in $\Delta\sigma$, 3 (FEA) *vs* 30 MPa (EA-MOD). In the EA method, extrapolation (log σ-$1/T$ relationship) over 24 °C results in an additional 17 MPa of σ correction compared to EA-MOD (σ-T relationship). For interpolation to $T_0 > 750$ °C, *i.e.*, 850 °C and above, where extrapolation is not required, the EA method gives lower $\Delta\sigma$ compared to EA-MOD as a result of the nonlinear relationship between σ and T in the former. For example, in Table V, for $\dot{\varepsilon} = 0.01\ s^{-1}$, $T_0 = 850$ °C, and $\varepsilon = 1$, the corresponding values of $\Delta\sigma$ are 2 (FEA), 14 (EA), and

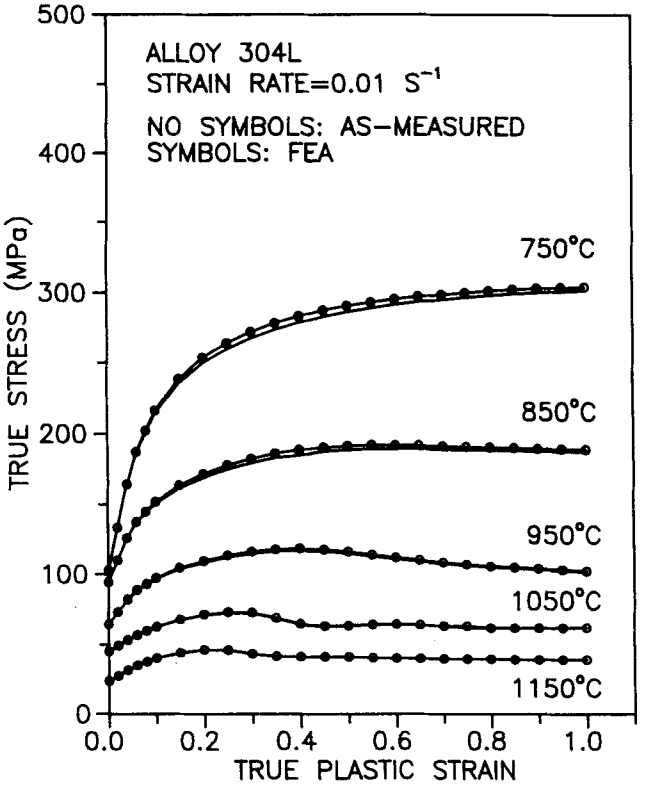

Fig. 10—True stress *vs* true plastic strain for alloy 304L compressed at a $\dot{\varepsilon}$ of 0.01 s^{-1}. The initial temperature of the tests ranged between 750 °C and 1150 °C. Curves without symbols are the as-measured behaviors. Curves with symbols (circles) are the predicted isothermal behaviors from the FEA method.

19 MPa (EA-MOD), where ΔT was 1.4 °C (FEA) and 15 °C (EA, EA-MOD). Again, a near 10-fold difference in ΔT results in a 10-fold difference in $\Delta\sigma$, comparing FEA to EA-MOD. The nonlinear correction in EA provides a smaller correction than might be expected from the differences in magnitude of ΔT calculated by the FEA and EA methods.

The close correspondence between the as-measured and FEA values of ΔT (Figure 4) demonstrates that the FEA method for obtaining $\sigma = \sigma(\varepsilon)|_{T_0,\dot{\varepsilon}}$ probably provides a better estimate of the true state of the isothermal behavior of alloy 304L compared to the EA method. The values and behavior of Q_{DEF}, calculated from both the as-measured and FEA-isothermal data, will be discussed. Although strain-rate sensitivity (m) is not discussed, it can be observed that values for an average m, calculated for a specific $\dot{\varepsilon}$ range from the data in Tables III through V, show that m is generally underestimated from the as-measured data. For example at T_0 = 950 °C and ε = 1, the average m value in the low strain-rate range, from 0.01 to 0.1 s^{-1}, is 0.17 from the as-measured data compared to 0.21 for the isothermal data. This undervaluation is due to relatively greater sample heating and associated flow softening at the higher $\dot{\varepsilon}$, of the $\dot{\varepsilon}$ pair, used to determine m.

IV. DISCUSSION

A. *Heat Retention Efficiency Term, η*

The heat retention efficiency η is assumed to vary linearly with log $\dot{\varepsilon}$ equaling 0 at $\dot{\varepsilon}$ = 0.001 s^{-1} and 0.95 at $\dot{\varepsilon}$ = 1 s^{-1},[29] as shown by Eq. [2] and graphically by the dashed line in Figure 11. For comparison, η was also calculated from the FEA data (Figures 5 through 7) by dividing the calculated ΔT by the maximum ΔT obtained for an adiabatic case. The latter value was obtained from Eq. [1], where η = 0.95, and the as-measured σ-ε data. The variation of η derived from FEA data is shown in Figure 11 for two levels of ε: 0.2 and 0.7. From the FEA data, it appears that η can be assumed to be equal to zero at 0.001 s^{-1} and 0.95 at 10 s^{-1} (rather than at 1 s^{-1}). The experimental data on aluminum,[28] shown in Figure 11, also supports this conclusion. The FEA data for 304L demonstrates that the variation of η with log $\dot{\varepsilon}$ is distinctly nonlinear. Also, it is shown that η depends distinctly on ε. Comparison of η from the two methods (Figure 11) shows that the linear approximation of η in the EA method gives significantly underestimated values of η at low ε, *e.g.*, for ε = 0.2, in the $\dot{\varepsilon}$ range from 0.01 to 0.5 s^{-1} and overestimated values at high ε, *e.g.*, for ε = 0.7, from 0.005 to 0.1 s^{-1}. The decrease in FEA η from 0.2 to 0.7 ε at constant $\dot{\varepsilon}$, observed in Figure 11, is due to changes in sample geometry, reducing thickness and increasing diameter, with increasing ε. Both

Table III. The As-Measured (MEAS), FEA Isothermal (ISO), and EA Isothermal (EA) Values of σ (MPa) for Various T_0, at 0.1 Increments of ε, and a $\dot{\varepsilon}$ of 1 s^{-1}*

	750 °C				850 °C				950 °C				1050 °C		1150 °C	
ε	MEAS	FEA	EA	EA-MOD	MEAS	FEA	EA	EA-MOD	MEAS	FEA	EA	EA-MOD	MEAS	FEA	MEAS	FEA
0.0	78.4	78.4	—	—	8.1	78.1	—	—	75.5	75.5	—	—	59.7	59.7	50.4	50.4
0.1	236	238	—	—	206	207	—	—	171	172	—	—	114	115	83.5	83.9
0.2	289	294	295	294	247	251	251	252	198	202	201	202	130	134	93.1	94.5
0.3	317	326	—	—	267	276	—	—	210	218	—	—	138	144	99.0	101
0.4	334	349	356	351	278	291	291	293	217	229	228	230	142	151	102	106
0.5	344	366	—	—	285	303	—	—	221	237	—	—	143	156	103	108
0.6	351	381	397	384	287	313	312	315	222	243	242	245	142	159	102	108
0.7	355	395	—	—	288	320	—	—	222	247	—	—	140	160	101	107
0.8	357	406	438	411	286	326	324	330	220	249	249	252	136	160	98.3	105
0.9	358	418	—	—	283	332	—	—	218	251	—	—	132	160	95.7	103
1.0	358	430	486	438	280	338	343	346	214	252	254	257	127	159	93.2	101

*Isothermal σ was also calculated with a modified EA method (EA-MOD), assuming that stress varies linearly with T_i, for interpolation of σ to T_0, rather than the assumed linear variation of log σ to $1/T_i$.

Table IV. The As-Measured (MEAS), FEA Isothermal (ISO), and EA Isothermal (EA) Values of Stress for Various Deformation Temperatures, at 0.1 Increments of ε, and a $\dot{\varepsilon}$ of 0.1 s^{-1}*

	750 °C				850 °C				950 °C				1050 °C		1150 °C	
ε	MEAS	FEA	EA	EA-MOD	MEAS	FEA	EA	EA-MOD	MEAS	FEA	EA	EA-MOD	MEAS	FEA	MEAS	FEA
0.0	96.6	96.6	—	—	84.0	84.0	—	—	78.4	78.4	—	—	58.0	58.0	35.7	35.7
0.1	233	235	—	—	192	193	—	—	134	135	—	—	87.9	88.7	57.1	57.4
0.2	278	284	284	282	222	226	222	225	150	155	150	154	99.0	101	64.4	65.3
0.3	300	311	—	—	236	245	—	—	158	166	—	—	104	108	68.3	69.7
0.4	313	329	334	326	243	256	253	254	163	174	170	172	106	110	67.6	69.5
0.5	320	342	—	—	246	263	—	—	165	177	—	—	104	110	64.3	66.6
0.6	325	350	360	350	247	266	263	267	164	178	175	178	99.3	106	61.5	63.9
0.7	328	356	—	—	247	268	—	—	161	176	—	—	95.4	102	60.0	62.3
0.8	331	360	390	371	246	268	271	276	157	172	174	178	92.8	99.5	58.7	60.8
0.9	333	363	—	—	244	267	—	—	153	168	—	—	90.6	96.7	57.4	59.4
1.0	335	363	418	388	246	267	282	288	150	164	173	180	89.0	94.4	56.7	58.4

*Isothermal σ was also calculated with a modified EA method (EA-MOD), assuming that stress varies linearly with T_i, for interpolation of σ to T_0, rather than the assumed linear variation of log σ to $1/T_i$.

Table V. The As-Measured (MEAS) and FEA Isothermal (ISO), Values of Stress for Various Deformation Temperatures, at 0.1 Increments of ε, and a $\dot{\varepsilon}$ of 0.01 s^{-1}*

	750 °C				850 °C				950 °C				1050 °C		1150 °C	
ε	MEAS	FEA	EA	EA-MOD	MEAS	FEA	EA	EA-MOD	MEAS	FEA	EA	EA-MOD	MEAS	FEA	MEAS	FEA
0.0	102	102	—	—	93.9	93.9	—	—	64.2	64.2	—	—	44.8	44.8	23.2	23.2
0.1	214	216	—	—	150	152	—	—	96.1	96.8	—	—	62.0	62.3	39.6	39.7
0.2	250	253	254	252	169	171	170	171	108	109	109	109	70.6	71.1	45.8	46.0
0.3	267	272	—	—	179	182	—	—	114	116	—	—	72.0	72.6	42.7	42.9
0.4	278	283	290	287	186	188	190	191	117	118	118	119	63.7	64.3	40.6	40.8
0.5	286	290	—	—	188	191	—	—	114	116	—	—	62.5	63.0	40.6	40.7
0.6	291	295	313	306	189	192	196	199	110	112	114	115	63.7	64.1	39.5	39.6
0.7	295	298	—	—	189	191	—	—	107	108	—	—	62.4	62.7	39.3	39.4
0.8	298	301	332	320	188	190	199	203	104	105	109	111	61.0	61.2	39.0	39.0
0.9	300	303	—	—	188	189	—	—	103	104	—	—	61.3	61.5	38.6	38.6
1.0	301	304	348	331	187	189	201	206	101	102	107	110	61.5	61.7	38.7	38.7

*Isothermal σ was also calculated with a modified EA method (EA-MOD), assuming that stress varies linearly with T_i, for interpolation of σ to T_0, rather than the assumed linear variation of log σ to $1/T_i$.

Table VI. Activation energy, Q_{DEF}, at Constant Stress and for Two Strain Levels, 0.2 and 0.6*

		Activation Energy (kJ/mole)							
		Variable							
		1 s^{-1}		0.1 s^{-1}		0.01 s^{-1}		Invariable	
Stress	(MPa)	MEAS	ISO	MEAS	ISO	MEAS	ISO	MEAS	ISO
100									
	Strain = 0.2	441	450	422	417	402	381	—	—
	Strain = 0.6	340	400	373	363	402	321	372	358
150									
	Strain = 0.2	470	469	399	394	312	302	—	—
	Strain = 0.6	408	389	386	347	364	300	386	346
200									
	Strain = 0.2	534	544	418	418	254	233	—	—
	Strain = 0.6	446	414	403	352	356	277	404	348
250									
	Strain = 0.2	609	658	471	488	271	204	—	—
	Strain = 0.6	478	457	423	366	361	245	422	358
300									
	Strain = 0.2	—	—	—	—	—	—	—	—
	Strain = 0.6	449	485	449	381	449	234	450	370
							Average =	407	356

*Values are shown for two assumptions: Q_{DEF} varies with $\dot{\varepsilon}$ or is constant over the entire $\dot{\varepsilon}$ range.

Table VII. Values for Peak Strain (ε_p) for Fine Grain 304L Tested at Various T_0-$\dot{\varepsilon}$ Pairs*

$\dot{\varepsilon}$	750 °C	850 °C	950 °C	1050 °C	1150 °C
0.01 s^{-1}					
As-measured	>1.0	0.60	0.40	0.26	0.23
Isothermal	>1.0	0.55	0.40	0.25	0.20
0.1 s^{-1}					
As-measured	>0.85	0.61	0.51	0.38	0.34
Isothermal	>1.0	0.75	0.56	0.44	0.35
1.0 s^{-1}					
As-measured	>0.86	0.65	0.61	0.51	0.50
Isothermal	>1.0	>1.0	>1.0	0.76	0.57

*Values from both as-measured and isothermal σ-ε data are given.

changes in geometry increase heat flow from the specimen to the dies, and as a result, the heat retention efficiency, η, is reduced with increasing ε. The effect of underestimation of η at low ε and overestimation at high ε in this $\dot{\varepsilon}$ range is that the EA calculated ΔT for the specimen is likewise under- and overestimated compared to the FEA values, as observed in Figures 6 and 7. Because calculated ΔT is used to correct the as-measured σ for deformational heating, the EA isothermal σ is likewise under- and overestimated for low and high ε, as shown in Tables IV and V.

B. *Observations Regarding Activation Energy for Deformation, Q_{DEF}*

The apparent activation energy for deformation, Q_{DEF}, appears in the equation attributed to Zener–Hollomon:[43]

$$Z = \dot{\varepsilon} \exp (Q_{DEF}/RT) \quad [3]$$

where T is the absolute temperature (in Kelvin), R is the universal gas constant, and Z is the Zener–Hollomon parameter. Zener and Hollomon suggest that flow stress is a function of Z and ε. For the calculation of Q_{DEF}, the following general expression for σ is assumed:

$$\sigma = f(\varepsilon)Z^u \quad [4]$$

where $f(\varepsilon)$ is some function of ε and u is a constant. The value of Q_{DEF} was calculated as a function of $\dot{\varepsilon}$ and T, for applied strains of 0.2 and 0.6, from both the as-measured and isothermal σ-ε data in Tables III through V. Figures 12 and 13 show the variation in σ, after an applied ε of either 0.2 or 0.6, respectively, with $1/T_0$ for the three strain rates studied. Each set of data was fitted to a third-order polynomial, and values of $1/T_0$ at constant σ were calculated for each $\dot{\varepsilon}$. Figures 14 and 15 show the variation of ln $\dot{\varepsilon}$ with $1/T_0$ for different σ levels. The slope of each curve corresponds to Q_{DEF}/R, from Eq. [3].

Because the 1150 °C test preheat resulted in a larger average grain diameter in the test specimen before deformation (0.12 *vs* 0.038 mm for the starting material), additional tests at 1150 °C were conducted to investigate the dependency of σ on grain size. Specimens were preheated at 1150 °C at either 1 or 8 hours, giving starting average grain diameters of 0.29 and 0.85 mm, respectively. Compression tests were then conducted at 0.01 and 1 s^{-1} at T_0 = 1150 °C. Grain size was found to have

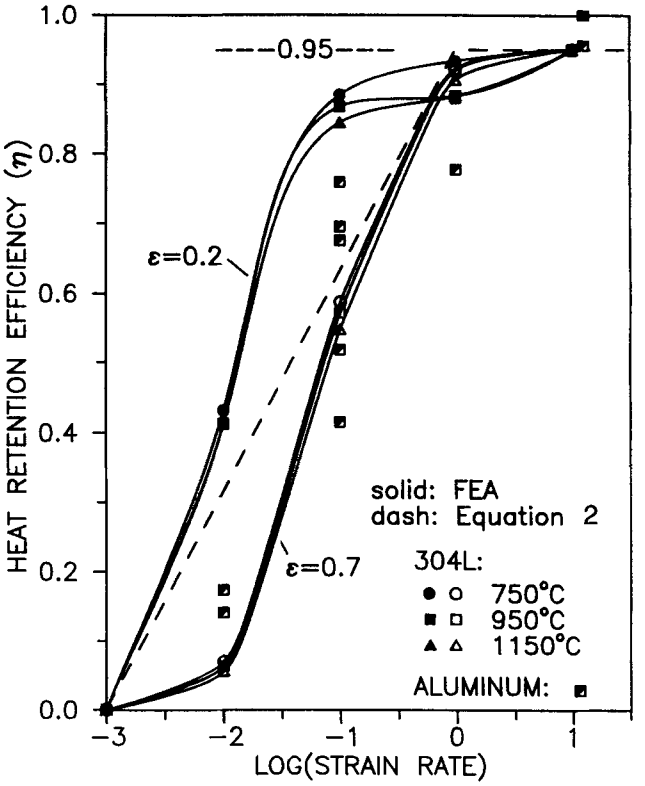

Fig. 11—Heat retention efficiency, η, *vs* log $\dot{\varepsilon}$ in the $\dot{\varepsilon}$ realm, where conventional-sized compression test samples of alloy 304L exhibit neither an isothermal nor an adiabatic state. The η from both methods, FEA and EA, are shown. Note, η calculated from FEA is dependent on strain. Data for aluminum is from Charpentier *et al.*[28]

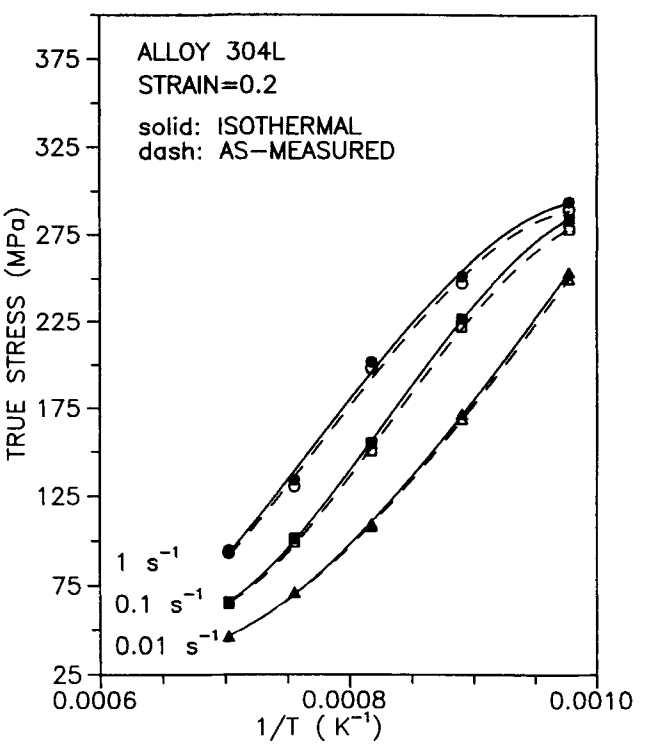

Fig. 12—The variation of true stress with inverse temperature (K^{-1}) for alloy 304L compressed at three different strain rates to a true strain of 0.2. Dashed curves are from the as-measured σ-ε data. The solid curves are from FEA isothermal data. Values of inverse temperature at various constant stress levels from this figure are used in Fig. 14.

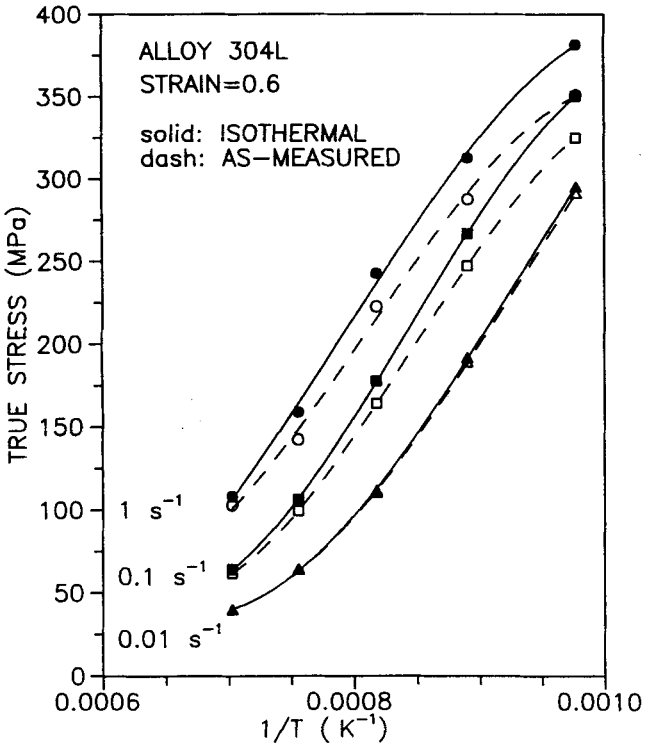

Fig. 13—The variation of true stress with inverse temperature (K^{-1}) for alloy 304L compressed at three different strain rates to a true strain of 0.6. Dashed curves are from the as-measured σ-ε data. The solid curves are from FEA isothermal data. Values of inverse temperature at various constant stress levels from this figure are used in Fig. 15.

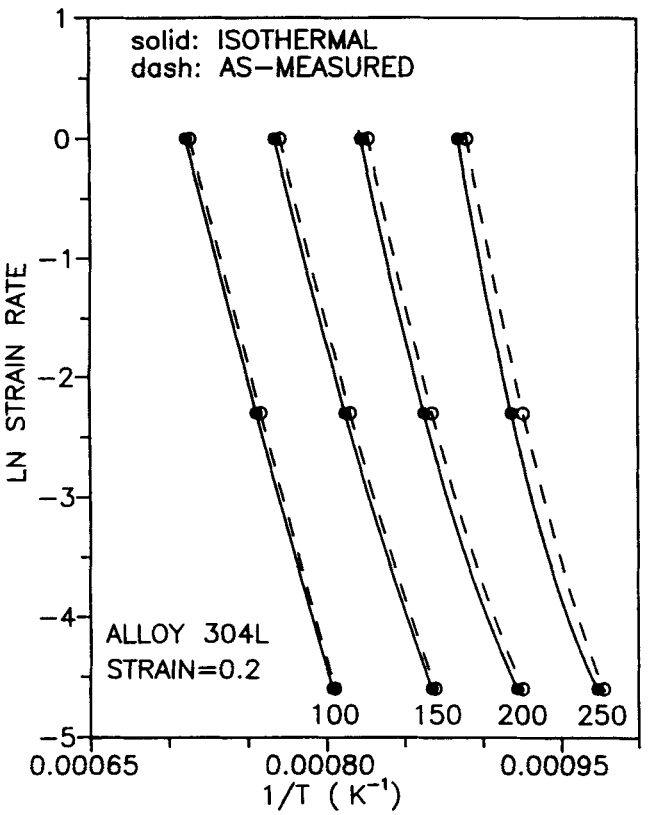

Fig. 14—The variation in natural logarithm of strain rate with inverse temperature (K^{-1}) at various constant stress levels (MPa) for alloy 304L compressed to a strain of 0.2. Dashed curves are from the as-measured σ-ε data. The solid curves are from FEA isothermal data.

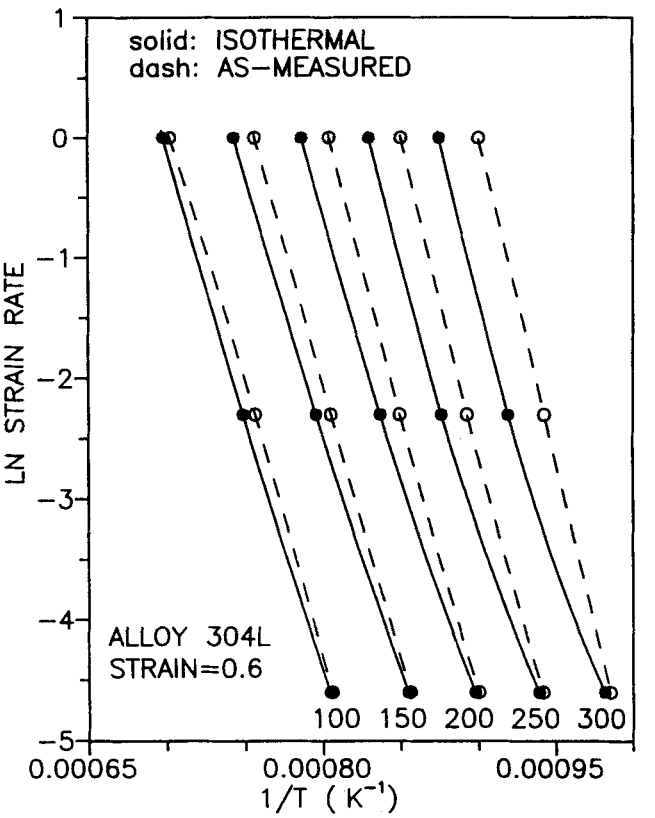

Fig. 15—The variation in natural logarithm of strain rate with inverse temperature (K^{-1}) at various constant stress levels (MPa) for alloy 304L compressed to a strain of 0.6. Dashed curves are from the as-measured σ-ε data. The solid curves are from FEA isothermal data.

little effect on the as-measured flow stress. For example, at $\dot{\varepsilon} = 1\ s^{-1}$ and $\varepsilon = 0.6$, σ was equal to 102, 99.4, and 103 MPa for average grain diameters of 0.12, 0.29, and 0.85 mm, respectively. At $\dot{\varepsilon} = 0.01\ s^{-1}$, the corresponding values of σ are 39.5, 39.8, and 42.6 MPa. Similar behavior is observed at $\varepsilon = 0.2$. Because of a lack of significant dependency of σ on grain size, the σ values from the 1150 °C tests are used in the calculation of Q_{DEF} that follows.

It has been common practice in the literature to calculate Q_{DEF} in the hot-working range from as-measured σ-ε data, probably because plots of ln $\dot{\varepsilon}$ with inverse T_0 generally exhibit a nearly linear behavior. Thus, Q_{DEF} is often assumed to be constant over the $\dot{\varepsilon}$ range studied. In fact, the as-measured data for 304L presented here and that presented for Cu[11] and Ni,[13] studied over a similar $\dot{\varepsilon}$ range, does indicate a constant Q_{DEF}. The assumption of constant Q_{DEF}, independent of T, $\dot{\varepsilon}$, and ε, is an attractive assumption, because it facilitates utilization of Z in the prediction of flow stress. However, the isothermal data in Figures 14 and 15 exhibits a distinct curvature that shows that Q_{DEF} decreases with decreasing $\dot{\varepsilon}$. Likewise, if the as-measured σ-ε data for Cu[11] and Ni[13] were corrected for adiabatic heating, Q_{DEF} would be shown to vary. A decreasing Q_{DEF} with decreasing $\dot{\varepsilon}$, in this $\dot{\varepsilon}$ range, is consistent with the general observation that Q_{DEF} in the creep realm has a lower value than in the hot-working realm. Evidence for a continuous variation of Q_{DEF} between these two realms is suggested here.

The data sets in Figures 14 and 15 were fitted with a second-order polynomial, and Q_{DEF} was calculated by differentiating the polynomial for the various deformation conditions (Table VI). At low ε, 0.2, values for Q_{DEF} from the as-measured and isothermal data are similar because of the limited amount of sample heating at low ε. The average Q_{DEF} obtained from the two sets of data is 417 and 413 kJ/mole, respectively. At a ε of 0.6, however, values of Q_{DEF} from as-measured and isothermal data are significantly different, 407 and 356 kJ/mole, respectively. In this case, significant heating of the sample occurs as a result of the greater applied ε. Samples deformed at the high $\dot{\varepsilon}$ retain most of the deformational heat, causing significant rise in T_i and decrease in σ as deformation proceeds. Thus, $1/T_i$ varies less with $\dot{\varepsilon}$ at constant σ (Figures 12 and 13) for the as-measured data compared to the isothermal data, yielding a reduced dependency of σ on T_i. This, in turn, results in a greater slope (Q_{DEF}/R) and higher values of Q_{DEF} from as-measured data in Figures 14 and 15. Thus, Q_{DEF} is overestimated from the as-measured data.

Figures 16 and 17 show the variation in Q_{DEF} with T (obtained from Table VI and Figures 14 and 15) for the three strain rates studied, at an applied ε of 0.2 and 0.6, respectively. At the lower ε (Figure 16), values for Q_{DEF} from the two sets of data, as-measured and isothermal, are very similar, as expected from the similarity of the σ-ε data. More importantly, Figure 16 shows that Q_{DEF} varies significantly with T and in a much different fashion, depending on $\dot{\varepsilon}$. For a $\dot{\varepsilon}$ of 1 s^{-1}, Q_{DEF} decreases with T. Conversely, at 0.01 s^{-1}, it increases. At 1100 K, Q_{DEF} for high and low $\dot{\varepsilon}$ have corresponding high and low values, 700 and 250 kJ/mole, respectively. At the intermediate $\dot{\varepsilon}$, 0.1 s^{-1}, Q_{DEF} first decreases and then increases with increase in T. The three curves appear to converge near a value of 400 kJ/mole as T approaches 1400 K.

Figure 17 shows that at a ε of 0.6, the variation in Q_{DEF} with T from the isothermal σ-ε data is well behaved, similar to the behavior shown in Figure 16 for lower ε. At 1100 K, Q_{DEF} increases significantly with $\dot{\varepsilon}$, having a value of 270 kJ/mole at the lowest rate and 525 kJ/mole at the highest. As T increases, Q_{DEF} for the three strain rates converges to a value of approximately 375 to 400 kJ/mole at 1400 K. In contrast, the variation in Q_{DEF} calculated from the as-measured σ-ε data (dashed curves in Figure 17) shows no consistent behavior.

Variations in the value of Q_{DEF} with $\dot{\varepsilon}$ could be attributed to a changing activity of the various dislocation mechanisms contributing to flow. For example, work-hardening moderated by cross slip is the dominant mechanism at high $\dot{\varepsilon}$ and low T. Dislocation climb and polygonization contribute to dynamic recovery at low $\dot{\varepsilon}$ and high T, similar to creep. A decrease in Q_{DEF} with an increase in T, similar to that observed in Figures 16 and 17 for a $\dot{\varepsilon}$ of 1 s^{-1}, is consistent with an increase in thermal activation for dislocations to overcome short-range barriers that obstruct their motion as T is raised. The increase in Q_{DEF} with T observed at the lowest $\dot{\varepsilon}$, 0.01 s^{-1}, indicates a decreasing dislocation mobility. For example, dislocation pinning by individual solute atoms

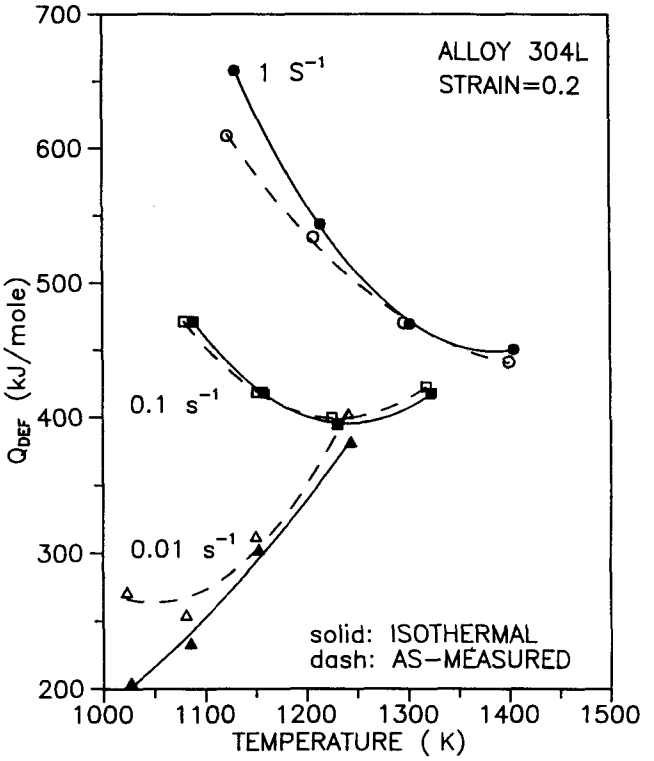

Fig. 16—The variation of activator energy, Q_{DEF}, with initial deformation temperature for alloy 304L compressed at three different strain rates to a strain of 0.2. Dashed curves are from the as-measured σ-ε data. The solid curves are from FEA isothermal data.

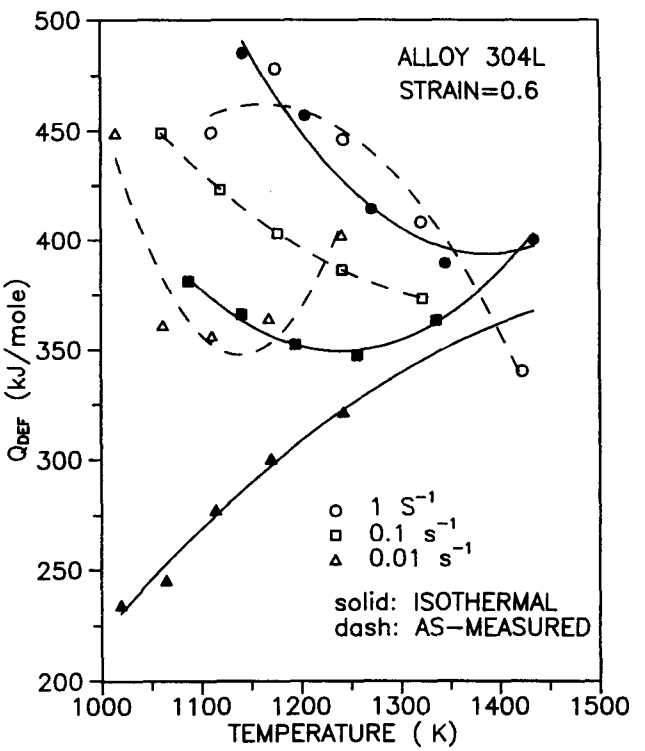

Fig. 17—The variation of activation energy, Q_{DEF}, with initial deformation temperature for alloy 304L compressed at three different strain rates to a strain of 0.6. Dashed curves are from the as-measured σ-ε data. The solid curves are from FEA isothermal data.

or atom complexes may become important at high T and low $\dot{\varepsilon}$. A similar increase in Q_{DEF} with T has been observed for creep of aluminum below $T/T_m = 0.5$, where T_m is the melting temperature (K), and at a $\dot{\varepsilon}$ of 3×10^{-11} s^{-1}.[44,45] The increase has been related to the transition from one deformation mechanism to another. At low T/T_m, creep in aluminum is controlled by dislocation intersection processes; at intermediate values by cross slip of screw dislocations; and at higher values, approaching 0.5, by dislocation climb and the nonconservative motion of jogs in screw dislocations. Above 0.5 T/T_m, creep is entirely diffusion controlled, and Q_{DEF} is relatively constant, increasing only slightly with T. However, as $\dot{\varepsilon}$ is increased to a value of 0.03 s^{-1}, a rate similar to the slowest used in this investigation, Q_{DEF} is shown to increase rapidly with T up to about 0.75 T/T_m. At the higher $\dot{\varepsilon}$, comparatively little time is available for diffusion-controlled processes, and the sensitivity of Q_{DEF} to T exhibited at low T/T_m is extended to higher T/T_m. The increase in Q_{DEF} with T for aluminum is similar to that observed here for 304L, both alloys deformed at equivalent $\dot{\varepsilon}$ and T/T_m.

The value of Q_{DEF} for $\dot{\varepsilon} = 0.01$ s^{-1} and $T = 1100$ K is 270 kJ/mole (Figure 17), which is significantly less than any of the values obtained by assuming an average linear behavior for the variation of Q_{DEF}/R for any σ level (Table VI) and is in fair agreement with the value of 314 kJ/mole reported for creep of alloy 304.[46] Similarly, Afonja[47] measured Q_{DEF} in a 23.6 Cr-5.12 Ni duplex stainless steel at a $\dot{\varepsilon} = 0.01$ s^{-1} and found the value, 242 kJ/mole, to agree with the activation energy reported for self-diffusion in similar Fe-Cr-Ni alloys. The Q_{DEF} for creep is generally equal to the activation energy for self-diffusion.[46] This suggests that Q_{DEF} for the creep realm may apply up to a $\dot{\varepsilon}$ of 0.01 s^{-1}, a few orders of magnitude above that considered to be the upper bound of the creep realm.

If the data in Figure 15 is assumed to behave in a linear fashion, Q_{DEF} from the isothermal data is relatively constant, varying little from the average value of 356 kJ/mole for different isostress levels. Conversely, Q_{DEF} from the as-measured data increases in a linear fashion from 372 kJ/mole at 100 MPa to 450 kJ/mole at 300 MPa. The assumption that Q_{DEF} can be obtained from as-measured σ-ε data probably accounts, in part, for the wide range of values of Q_{DEF} that have been reported for this alloy system (ranging from 393 to 600 kJ/mole).[30]

V. CONCLUSIONS

1. Deformational heating of laboratory-sized compression samples during testing in a $\dot{\varepsilon}$ range from 0.01 to 1 s^{-1}, at temperatures from 750 °C to 1150 °C, and to a ε of 1 can lead to significant stress softening and discrepancy between as-measured and isothermal σ-ε behaviors.
2. The FEA method presented provides an effective technique to calculate the instantaneous temperature of the compression sample, which coupled with the as-measured σ-ε values obtained from tests at different starting temperatures allows the determination of isothermal σ-ε. The FEA model predictions closely approximate measured temperature variations in the test sample during compression testing.
3. A conventional technique used to calculate instantaneous sample temperature (*via* Eqs. [1] and [2]) relies on η, a heat retention efficiency term that varies only with $\dot{\varepsilon}$, $\eta = \eta(\dot{\varepsilon})$, to reduce the heating calculated for an adiabatic condition. The FEA results show that η is also a function of ε, $\eta = \eta(\dot{\varepsilon}, \varepsilon)$, and the use of η in the simple sense can lead to significant errors in the calculated instantaneous sample temperature and resulting isothermal σ-ε behavior.
4. The apparent activation energy for deformation, Q_{DEF}, for 304L, calculated from the isothermal σ-ε data, decreases with decreasing $\dot{\varepsilon}$ in the range 0.01 to 1 s^{-1}. This behavior is consistent with the general observation that Q_{DEF} has a lower value in the creep range than in the hot-working range and suggests a smooth transition in the value of Q_{DEF} from one range to the other. Utilization of the as-measured σ-ε data, without correction for deformational heating, indicates that Q_{DEF} is constant in this $\dot{\varepsilon}$ regime. Values for Q_{DEF} from isothermal data are generally lower than those calculated from as-measured data.

ACKNOWLEDGMENTS

This work was performed under contract with the United States Department of Energy. The authors would like to acknowledge the technical support received from Michael Riendeau and Gary Coubrough, during mechanical testing. The authors would also like to acknowledge Michael Weis, Graduate Student, Advanced Steel Processing and Products Research Center, Colorado School of Mines, Golden, CO, for help in constructing the compression testing system.

REFERENCES

1. S. Kobayashi, S.I. Oh, and T. Altan: *Metal Forming and the Finite-Element-Method*, Oxford University Press, New York, NY, 1989.
2. C.R. Boer, N. Rebelo, H. Rydstad, and G. Schroder: *Process Modelling of Metal Forming and Thermomechanical Treatment*, Springer-Verlag, Heidelberg, 1986.
3. I. Haque, J.E. Jackson, Jr., T. Gangjee, and A. Raikar: *J. Mater. Shaping Technol.*, 1987, vol. 5 (1), pp. 23-33.
4. K.J. Meltsner: in *Simulation and Theory of Evolving Microstructures and Textures*, M.P. Anderson and A. Rollet, eds., TMS, Warrendale, PA, 1990.
5. A.J.M. Shih and H.T.Y. Yang: *Int. J. Numei*, 1991, vol. 31, pp. 345-67.
6. S.I. Oh, G.D. Lahoti, and T. Altan: in *Process Modeling Tools*, Proc. Soc. for Metals Process Modeling Sessions, Materials and Processes Congress, 1980, ASM, Metals Park, OH, 1981, pp. 195-216.
7. S.L. Semiatin, G.D. Lahoti, and T. Altan: in *Process Modeling: Fundamentals and Applications to Metals*, T. Altan, ed., ASM, Metals Park, OH, 1980, p. 387.
8. D.W. Livesey and C.M. Sellars: *Mater. Sci. Technol.*, 1985, vol. 1, pp. 136-44.
9. J.R. Douglas and T. Altan: *ASME Trans. J. Eng. Industry*, 1975, Feb., p. 66.
10. K.P. Rao, S.M. Doraivelu, and V. Gopinathan: *J. Mech. Work. Technol.*, 1982, No. 6, pp. 63-88.
11. V.M. Sample, G.L. Fitzsimons, and A.J. DeArdo: *Acta Metall.*, 1987, vol. 35 (2), pp. 367-79.

12. J.J. Jonas and T. Sakai: in *Deformation Processing and Structure*, G. Krauss, ed., ASM, Metals Park, OH, 1982, pp. 185-230.
13. J.J. Luton and C.M. Sellars: *Acta Metall.*, 1969, vol. 17, pp. 1033-43.
14. M.R. Staker and N.J. Grant: *Mater. Sci. Eng.*, 1985, No. 75, pp. 137-50.
15. V.M. Sample and L.A. Lalli: *Mater. Sci. Technol.*, 1987, vol. 3, pp. 28-35.
16. R. Raj: *Metall. Trans. A*, 1981, vol. 12A, pp. 1089-97.
17. C. Gandhi: *Metall. Trans. A*, 1982, vol. 13A, pp. 1233-38.
18. W. Roberts, H. Boden, and B. Ahlblom: *Met. Sci.*, 1979, Mar.-Apr., pp. 195-205.
19. M.J. White and W.S. Owen: *Metall. Trans. A*, 1980, vol. 11A, pp. 597-604.
20. J.J. McQueen, G. Gurewitz, and S. Fulop: *High Temp. Technol.*, 1983, Feb., pp. 131-38.
21. L.A. Norstrom: *Scand. J. Metall.*, 1977, vol. 6, pp. 269-276.
22. N. Cederblad and N.J. Grant: *Metall. Trans. A*, 1975, vol. 6A, pp. 1547-52.
23. W. Roberts and B. Ahlblom: *Acta Metall.*, 1978, vol. 26, pp. 801-13.
24. H.J. McQueen: *Metall. Trans. A*, 1977, vol. 8A, pp. 807-24.
25. A. Laasraoui and J.J. Jonas: *Metall. Trans. A*, 1991, vol. 22A, pp. 151-60.
26. A. Laasraoui and J.J. Jonas: *Metall. Trans. A*, 1991, vol. 22A, pp. 1545-58.
27. P. Dadras and J.F. Thomas, Jr.: *Metall. Trans. A*, 1981, vol. 12A, pp. 1867-73.
28. P.L. Charpentier, B.C. Stone, S.C. Ernst, and J.F. Thomas, Jr.: *Metall. Trans. A*, 1986, vol. 17A, pp. 2227-37.
29. J.F. Thomas, Jr. and R. Srinivasan: in *Computer Simulation in Materials Science*, R.J. Arsenault, J.R. Beeler, Jr., and D.M. Esterling, eds., ASM INTERNATIONAL, Metals Park, OH, 1988, pp. 269-90.
30. M.C. Mataya, E.L. Brown, and M.P. Riendeau: *Metall. Trans. A*, 1990, vol. 21A, pp. 1969-87.
31. P. Dadras: *J. Eng. Mater. Technol.*, 1985, vol. 107, pp. 97-100.
32. S.L. Semiatin and J.H. Holbrook: *Metall. Trans. A*, 1983, vol. 14A, pp. 1681-95.
33. M.C. Mataya and D.K. Matlock: in *Superalloy 718-Metallurgy and Applications*, E. Loria, ed., TMS, Warrendale, PA, 1989, pp. 155-78.
34. W. Reiss and K. Pohlandt: *Exp. Tech.*, 1986, Jan., pp. 20-24.
35. M.J. Weis: Master's Thesis, Colorado School of Mines, Golden, CO, 1987.
36. G.W. Rowe: *An Introduction to the Principles of Metalworking*, Edward Arnold, London, 1965, p. 245.
37. G.E. Dieter: *Mechanical Metallurgy*, 2nd ed., McGraw-Hill, Inc., New York, NY, 1976, pp. 72-102.
38. K.F. Kennedy and G.D. Lahoti: Battelle Columbus Laboratories, Columbus, OH, private communication, June 1981.
39. D.R. Barraclough and C.M. Sellars: *Met. Sci.*, 1979, Mar.-Apr., pp. 257-67.
40. H. Suzuki, Y. Hashizume, Y. Yabuki, Y. Ichihara, S. Nakajima, and K. Kenmochi: *Report of the Institute of Industrial Science of the University of Tokyo*, 1968, vol. 18 (3), pp. 1-102.
41. C.M. Sellars: *Proc. Conf. on Hot Working and Forming Processes*, Sheffield, July 1979, Metals Society, London, 1980, pp. 3-15.
42. J.J. Jonas and H.J. Mcqueen: *Treatise on Materials Science and Technology: Plastic Deformation of Materials*, R.J. Arsenault, ed., Academic Press, New York, NY, 1975, vol. 6, pp. 394-490.
43. C. Zener and J.H. Hollomon: *J. Appl. Phys.*, 1944, vol. 15, pp. 22-31.
44. O.D. Sherby and P.M. Burke: in *Progress in Materials Science*, B. Chalmers and W. Hume-Rothery, eds., Pergamon Press, London, 1968, vol. 13, pp. 325-53.
45. H. Luthy, A.K. Miller, and O.D. Sherby: *Acta Metall.*, 1980, vol. 28, pp. 169-78.
46. H.J. McQueen: *J. Met.*, 1968, Apr., pp. 31-38.
47. A.A. Afonja: *Mater. Sci. Eng.*, 1982, No. 54, pp. 257-63.